https://doi.org/10.5194/egusphere-2025-3040
Preprint. Discussion started: 14 August 2025

Sensitivity of tunable infrared laser spectroscopic measurements of $\Delta'^{17}O$ in CO_2 to analytical conditions

David Bajnai[1], Vincent J. Hare[2,3]

[1]Department of Geochemistry and Isotope Geology, Geoscience Center Göttingen, University of Göttingen, Göttingen, Germany
[2]Stable Light Isotope Laboratory, Department of Archaeology, University of Cape Town, Cape Town, South Africa
[3]Node for Isotope Biogeochemistry, BIOGRIP, University of Cape Town, Cape Town, South Africa

Correspondence to: David Bajnai (david.bajnai@uni-goettingen.de)

Abstract.

Triple oxygen isotope ($\Delta'^{17}O$) measurements of CO_2 are increasingly used in paleoenvironmental and atmospheric sciences, in part due to the emergence of tunable infrared laser direct absorption spectroscopy (TILDAS) as a cost- and time-effective method for quantifying rare isotopologues in CO_2. This study aims to provide users with a clear understanding of how the stability of analytical conditions — such as optical cell temperature, pressure, and CO_2 concentration — affects measurement quality. Using data from two laboratories equipped with TILDAS instruments (University of Göttingen and University of Cape Town), both operating in high-precision dual-inlet mode, we demonstrate how variations in these parameters influence measurement repeatability and long-term stability. The most significant factor affecting short-term repeatability of $\Delta'^{17}O$ is a mismatch in CO2 concentration between sample and working standard. The resulting scale-offset effect can amount to several ppm per 1 µmol mol mismatch, depending on instrumental parameters. We show that empirical corrections for such offsets, arising from variable pCO_2 of the analyte across measurements, significantly improve reproducibility. In contrast, the dominant influence on long-term stability is drift in optical cell temperature and pressure. In air monitoring studies, unrecognized instrumental drift due to variations in optical cell temperature, pressure, and CO_2 concentrations can be misinterpreted as genuine seasonal variations in $\Delta'^{17}O$. We conclude with practical recommendations for achieving the highest possible precision with TILDAS, emphasizing that continuous monitoring and reporting of analytical conditions is essential.

1 Introduction

The analysis of all three stable oxygen isotopes (^{16}O, ^{17}O, and ^{18}O, referred to as "triple oxygen isotope" analyses) in CO_2 is a rapidly growing field thanks to recent advances in methodology. For example, the combined analyses of $\delta^{18}O$ and $\delta^{17}O$ in atmospheric CO_2 provides a tracer for the global carbon cycle (Hoag et al., 2005; Horváth et al., 2012; Koren et al., 2019; Liang et al., 2023; Steur et al., 2024; Thiemens et al., 2014). Triple oxygen isotope analyses of carbonate-derived CO_2 has

https://doi.org/10.5194/egusphere-2025-3040
Preprint. Discussion started: 14 August 2025

been used to reconstruct past environmental conditions (Affek et al., 2023; Kelson et al., 2022; Sha et al., 2024; Wostbrock et al., 2024) and study (bio)mineralization processes (Arduin-Rode et al., 2024; Bajnai et al., 2024).

Mass-dependent fractionation processes result in a correlation between the $\delta^{17}O$ and $\delta^{18}O$ values, following slopes of approximately 0.5 (Craig, 1957; Luz and Barkan, 2010; Matsuhisa et al., 1978; Young et al., 2002). The exact slope of the correlation depends on the specific mass dependent fractionation process and temperature. The $\Delta'^{17}O$ notation expresses deviations in the relative abundances of oxygen isotopes from a reference line, enabling distinguishing between various fractionation mechanisms:

$$\Delta'^{17}O = \ln(\delta^{17}O + 1) - \lambda_{RL} \cdot \ln(\delta^{18}O + 1) - \gamma_{RL} \quad \text{Eq. (1)}$$

where λ_{RL} and γ_{RL} represent the slope and intercept of the reference line, respectively. Following common practice, we use $\lambda_{RL} = 0.528$ and $\gamma_{RL} = 0$ (Luz and Barkan, 2010; Miller et al., 2020).

Stable carbon and oxygen isotope ratios ($\delta^{13}C$ and $\delta^{18}O$) in CO_2 are typically measured using isotope ratio mass spectrometry (McCrea, 1950). However, the isotopologue $^{16}C^{13}C^{16}O$ has the same nominal mass as the most abundant ^{17}O-containing isotopologue $^{16}O^{12}C^{17}O$. This mass interference not only prevents the direct measurement of $\delta^{17}O$ in CO_2 using conventional mass spectrometry but also necessitates corrections in these measurements to account for the ^{17}O signal (Brand et al., 2010; Petersen et al., 2019). To generate $\Delta'^{17}O$ data for carbonates and CO_2, alternative approaches have been developed, most of which produce O_2 as the analyte, thereby avoiding mass interference. These techniques include the fluorination of CO_2 or carbonate (Wostbrock et al., 2020), the conversion of CO_2 to H_2O followed by the fluorination of H_2O using CoF_3 (Brenninkmeijer and Röckmann, 1998; Passey et al., 2014), the equilibration of CO_2 with O_2 using a Pt catalyst (Barkan and Luz, 2012; Mahata et al., 2013), and the equilibration of CO_2 with CeO_2 followed by fluorination (Hofmann and Pack, 2010; Mahata et al., 2012). High-resolution mass spectrometry has also been used to obtain precise $\Delta'^{17}O$ data on CO_2 (Adnew et al., 2019).

In recent years, laser spectroscopy has become a viable alternative to mass spectrometry for quantifying rare isotopologues in a range of trace gases, such as CO_2, N_2O, and CH_4 (McManus et al., 2006; Mohn et al., 2014; Nataraj et al., 2022; Nelson et al., 2008; Prokhorov et al., 2019; Sakai et al., 2017; Stoltmann et al., 2017; Tuzson et al., 2008; Wang et al., 2020; Yanay et al., 2022; Zhang et al., 2025). Laser spectroscopy determines isotopologue abundances based on the absorption of laser light at specific wavelengths that correspond to the unique vibrational and rotational energy levels of different isotopologues. Consequently, isotopologue ratios obtained through laser spectroscopy are inherently free from mass interference-related biases. For triple oxygen isotope measurements in CO_2, two different spectroscopy techniques have been used, cavity ring-down spectroscopy (CRDS) (Chaillot et al., 2025; Stoltmann et al., 2017), and tunable infrared laser direct absorption spectroscopy (TILDAS) (Bajnai et al., 2023; Hare et al., 2022; Perdue et al., 2022; Steur et al., 2021). In this paper, we specifically focus on TILDAS. While some aspects of our discussion relate to the commercially available TILDAS instrument

https://doi.org/10.5194/egusphere-2025-3040
Preprint. Discussion started: 14 August 2025

from Aerodyne Research Inc. (Billerica, MA, USA), which also has been used in several recent studies on CO_2 triple oxygen isotopes, most apply to the technique in general.

A typical TILDAS setup consists of a quantum cascade laser with a tunable output frequency, a multi-pass cell containing the analyte gas, and a detector (McManus et al., 2006, 2015; Nelson et al., 2008). The Beer-Lambert Law provides the foundation for calculating isotopologue abundances:

$$I_{(\nu)} = I_{o\,(\nu)} \exp\left[-\frac{N_A}{ln(10)}\, S_{(T)}\, \phi_{(\nu,P,T)}\, L\, C\right] \quad \text{Eq. (2)}$$

where I and I_0 are the intensity of the transmitted and the incident light at frequency ν, respectively. N_A is Avogadro's number (molecules mol^{-1}), S denotes the line strength (cm^{-1} (molecule $cm^{-2})^{-1}$), which depends on temperature, ϕ the line-shape function (cm), L the absorption path length (cm), and C the concentration of the absorbing species (mol cm^{-3}). For CO_2 triple oxygen isotope measurements, the abundance of the isotopologues "628" ($^{16}O^{12}C^{18}O$), "627" ($^{16}O^{12}C^{17}O$), and "626" ($^{16}O^{12}C^{16}O$) are quantified based on respective, distinct absorption peaks in the spectral region around 2349 cm^{-1} (Fig. 1). These shorthand notations, commonly used in spectroscopy, identify isotopologues by the second digit of the atoms' atomic masses. The line shape function describes how the absorption of light is distributed around the central wavenumber of a spectral line. It is typically represented by Voigt profile and is derived empirically from the acquired absorption spectra, measurements of temperatures and pressure as well as spectroscopic fitting parameters retrieved from the high-resolution transmission molecular absorption database (HITRAN) (Gordon et al., 2022).

Several studies have demonstrated that TILDAS can achieve a repeatability of $\Delta'^{17}O$ measurements of 10 ppm or better, measured as the standard error from multiple replicate analyses of the same analyte (Bajnai et al., 2023; Hare et al., 2022; Perdue et al., 2022). While variations in the analytical conditions, such as temperature, pressure, and concentration have been shown to influence the repeatability of $\Delta'^{17}O$ measurements by TILDAS (Bajnai et al., 2023; Hare et al., 2022, 2025; Perdue et al., 2022), the extent to which they affect the measured values remain largely unexplored. Minimizing analytical errors is becoming increasingly critical for $\Delta'^{17}O$ measurements as its applicability is expanded in long-term atmospheric monitoring studies (Steur et al., 2024) and the investigations of sub-10 ppm fractionation effects (Bajnai et al., 2024). In this paper, we examine the sources of analytical uncertainties in two TILDAS setups, located at the University of Göttingen and the University of Cape Town, and evaluate how variations in analytical conditions affect the repeatability of triple oxygen isotope ($\Delta'^{17}O$) measurements of CO_2.

2 Definitions of spectroscopic isotopologue ratios

TILDAS instruments report scaled isotopologue mole fractions, also referred to as mixing ratios (χ', commonly expressed as μmol mol^{-1} but Aerodyne Research Inc. instruments report nmol mol^{-1}):

https://doi.org/10.5194/egusphere-2025-3040
Preprint. Discussion started: 14 August 2025

$$\chi'_{\mathrm{i}} = C_{\mathrm{i}}\, R\, \frac{T}{P}\, \frac{1}{X_{\mathrm{i}}} \qquad \text{Eq. (3)}$$

where C is the concentration (mol m^{-3}) of the isotopologue i (e.g., "626", "627", "628"), R is the gas constant (m^3 Pa K^{-1} mol^{-1}), T and P denote the temperature (K) and pressure (Pa) of the analyte gas, respectively. X_{i} denotes the isotopologue abundance of the analyzed isotopologue, as defined in the HITRAN database: X_{626} = 0.98420, X_{628} = 0.0039471, and X_{627} = 0.000734 (De Biévre et al., 1984; Gordon et al., 2022). Each isotopologue absorption feature is scaled by the corresponding line strength in the HITRAN database and the reference isotopic abundances. Consequently, the mixing ratios in Eq. (3) are effectively normalized to the total concentration of all isotopologues at natural abundance. Expressing isotopologue abundances as mixing ratios facilitates the calculation of the δ-values (c.f., Griffith et al., 2012; Hare et al., 2022):

$$\delta^{17}\mathrm{O}_{\mathrm{meas}} = \frac{\chi'_{627}}{\chi'_{626}} - 1 \quad \text{and} \quad \delta^{18}\mathrm{O}_{\mathrm{meas}} = \frac{\chi'_{628}}{\chi'_{626}} - 1 \qquad \text{Eq. (4)}$$

The scale of these measured δ-values is based on the natural isotopologue abundances used in HITRAN and need to be corrected for instrumental drift. This is done similarly as in isotope ratio mass spectrometry, by repeated alternating measurements of sample ("smp") and a working standard ("std"), and reporting δ-values relative to the working standard (McKinney et al., 1950):

$$\delta^{17}\mathrm{O}_{\mathrm{smp/std}} = \frac{\delta^{17}\mathrm{O}^{\mathrm{meas}}_{\mathrm{smp}} + 1}{\delta^{17}\mathrm{O}^{\mathrm{meas}}_{\mathrm{std}} + 1} - 1 \quad \text{and} \quad \delta^{18}\mathrm{O}_{\mathrm{smp/std}} = \frac{\delta^{18}\mathrm{O}^{\mathrm{meas}}_{\mathrm{smp}} + 1}{\delta^{18}\mathrm{O}^{\mathrm{meas}}_{\mathrm{std}} + 1} - 1 \qquad \text{Eq. (5)}$$

As in isotope-ratio mass spectrometry, instrumental drift is mitigated by bracketing each sample analysis with measurements of a working standard. This approach relies on the assumption that changes in analytical conditions affect both the sample and the standard equally, and that sample and working standard have similar molecular composition (i.e, they are matrix-matched).

3 Dependence of the measured Δ'^{17}O values on the analytical conditions

3.1 Analytical setups

University of Göttingen and the University of Cape Town are both equipped with TILDAS instruments from Aerodyne Research Inc. (Billerica, MA, USA), each coupled with custom-built inlet systems. The design and operation of these systems are described in detail by Bajnai et al. (2023) and Hare et al. (2022). In both laboratories, a single replicate measurement consists of multiple sample cycles bracketed by measurements of a working standard (Eq. 5). However, differences in the inlet systems result in slightly differing analytical procedures.

In TILDAS, mixtures of CO_2 and a collision gas (e.g., CO_2-free air or pure N_2) are used to enhance optical signals at low cell pressures (< 50 Torr). For reproducible measurements, CO_2 must be thoroughly mixed in the collision gas (c.f., Hare et al.,

https://doi.org/10.5194/egusphere-2025-3040
Preprint. Discussion started: 14 August 2025

2022). However, matching the CO_2 concentration of the sample to that of the working standard, typically within 1 µmol mol^{-1} can be challenging. A key distinction between the setups at Göttingen and Cape Town lies in how the mismatch between the sample and standard analyte's CO_2 concentrations are handled. At Göttingen, the χ'$_{626}$ of sample and working standard are kept within ±1 ppm of each other within a replicate (Fig. 2a), and subsequent replicate analyses are also kept within ±1 ppm. This is achieved by mixing pure CO_2 analytes, for both reference and sample, with a bathing (collision) gas to a predefined target prior to each respective measurement cycle. In contrast, at Cape Town, the reference gas is pre-mixed and taken from a 50 L high pressure cylinder of 421 µmol mol^{-1} CO_2 in Nitrogen 5.0, resulting in identical χ'$_{626}$ values of the working standard across replicate analyses within 0.1 µmol mol^{-1} (1σ). The χ'$_{626}$ of the sample, however, varies from sample to sample, depending on the amount of sample gas available for analysis (Fig. 2b).

3.2 Concentration dependence due to scale-offset

The effect of mismatched CO_2 concentrations between sample and working standard have been shown to be substantial and require correction (Bajnai et al., 2023; Hare et al., 2022, 2025; Steur et al., 2024). In the following, we explain how this effect arises and present a general correction scheme for cases where sample and working standard concentrations are mismatched.

The total mole fraction of CO_2 in a gas mixture (pCO_2) equals the sum of mole fractions from all isotopologues, including multiply substituted species. Current measurement techniques cannot simultaneously detect every isotopologue, so the true pCO_2 of the analyte cannot be accurately determined. Because χ' values are reported in a way to estimate pCO_2 (Eq. 3), measured χ' values may deviate from the "true" mole fractions of the analyte gas (c.f., Griffith et al., 2012; Hare et al., 2022):

$$\chi'^{\text{true}}_{627} = a_{627} \cdot \chi'_{627} + b_{627} \qquad \text{Eq. (6)}$$

where a_{627} and b_{627} are scaling factors which relate the measured isotopologue mole fractions to the "true" isotopologue mole fractions. Similar equations can be written for χ'$_{626}$ and χ'$_{628}$.

Using Eq. (6), we can describe a more accurate form of Eq. (4), adjusted for the offsets:

$$\delta^{17}\mathrm{O}_{\text{true}} = \frac{a_{627} \cdot \chi'_{627} + b_{627}}{a_{626} \cdot \chi'_{626} + b_{626}} - 1 \quad \text{and} \quad \delta^{18}\mathrm{O}_{\text{true}} = \frac{a_{628} \cdot \chi'_{628} + b_{628}}{a_{626} \cdot \chi'_{626} + b_{626}} - 1 \qquad \text{Eq. (7)}$$

An equivalent of Eq. (7) can be written using only the measured δ-values and χ'$_{626}$ (see Eq. 4 in Hare et al., 2022):

$$\delta^{17}\mathrm{O}_{\text{true}} = \delta^{17}\mathrm{O}_{\text{meas}} \cdot \frac{\chi'_{626} \cdot a_{627}}{\chi'_{626} \cdot a_{626} + b_{626}} + \frac{\chi'_{626} \cdot (a_{627} - a_{626}) + b_{627} - b_{626}}{\chi'_{626} \cdot a_{626} + b_{626}} \qquad \text{Eq. (8)}$$

Equation (8) implies that all δ-values, and consequently Δ'^{17}O values, measured by spectroscopy depend on the measured mole fraction of the most abundant CO_2 isotopologue, χ'$_{626}$. In practical terms this means, that variations in χ'$_{626}$ across successive measurement cycles within a replicate or across individual replicate analyses would influence measurement repeatability.

https://doi.org/10.5194/egusphere-2025-3040
Preprint. Discussion started: 14 August 2025

To correct for pCO_2 mismatch, the "true", scale-offset-corrected δ-values need to be determined. In practical terms, this means that the constants a and b in Eq. (7) need to be known. Instead of correcting the δ-values values, it is convenient to perform the correction on the measured $\Delta'^{17}O$ values directly. By combining Eqs (1, 4, 5, 7) and noting that $|b_{626}| << \chi'_{626}$, we can derive a correction scheme for $\Delta'^{17}O_{smp/std}$ values relative to the working standard used for bracketing. Note that this scheme is only valid for small differences in χ'_{626} between sample and standard:

$$\Delta'^{17}O^{true}_{smp/std} \simeq \Delta'^{17}O_{smp/std} - m \cdot \left(\chi'^{smp}_{626} - \chi'^{std}_{626}\right) \quad \text{Eq. (9)}$$

The correction slope m, defined as $(1- \lambda_{RL}) * a_{626} / b_{626}$, can be determined empirically. To do this, we carried out a series of experiments at Cape Town, in which 10 mg of IAEA-603 was reacted in 100% phosphoric acid at 70 °C and then diluted with varying amounts of N_2. This resulted in χ'^{smp}_{626} ranging from 360 µmol mol^{-1} to 435 µmol mol^{-1}, while the χ'^{std}_{626} was held constant at 421 µmol mol^{-1}. A similar experiment was done by diluting the working reference gas. A fit to this data — measured within the same analytical session (10–12 March, 2025) — yields a slope of m = -6 ppm per µmol mol^{-1} mismatch (χ'^{smp}_{626} - χ'^{std}_{626}), both for IAEA-603 and for the zero enrichment measurements (Fig. 3). This indicates that the correction is independent of the isotopic composition of the sample analyte. A second set of experiments conducted during a separate analytical session (21 November – 10 December 2024) yielded a slightly different slope for IAEA-603 of m = -7 ppm per µmol mol^{-1} mismatch (Fig. 3). This suggests that the correction slope varies slightly between sessions, likely in response to changing instrumental parameters, such as the laser tuning rate, the instrument purging rate, etc.

We apply the correction described above to address the mismatch between the pCO_2 of the sample and the working standard in the Cape Town dataset. Before correction, the (external) 1 standard deviation of the Cape Town NBS-18 and IAEA-603 $\Delta'^{17}O$ values is 110 ppm and 98 ppm, respectively, over the entire measurement period (Fig. 4a). After applying apply a scale-offset correction to the entire dataset, these values improve significantly, to 32 ppm and 38 ppm (Fig. 4b). Applying a session-specific correction (i.e. with different m fitted to each analytical session), there is further improvement to 20 ppm for both NBS-18 and IAEA-603 (see details in Hare et al., 2025).

Interestingly, the correction slopes m acquired in Cape Town is similar in value but opposite in sign compared to the mismatch experiments carried out in the University of Göttingen (Fig. 3; Bajnai et al. (2023)). A negative slope m is explained by positive values of a_{626}/b_{626} (for Cape Town), and vice versa (for Göttingen). This suggests that m, that is ultimately a_{626} and b_{626} may be instrument dependent, as well as session dependent.

We briefly note that other techniques, e.g., CRDS, use pure CO_2 gases instead of gas mixtures (c.f., Chaillot et al., 2025). According to Eq. (9), pure CO_2 implies that (χ'^{smp}_{626} - χ'^{std}_{626}), and hence m = 0, eliminating the need for such a correction.

https://doi.org/10.5194/egusphere-2025-3040
Preprint. Discussion started: 14 August 2025

3.3 Uncertainties introduced by empirical fitting of the line shape function

Because the line shape function is empirically derived from the absorption spectra, the calculated concentrations are inherently subject to some inaccuracy (Eq. 2). The empirical fit may not fully capture subtle variations in thermal or collisional peak broadening, resulting in residual temperature and pressure dependencies in the measured concentrations. These biases can affect each spectral peak — and therefore each measured mixing ratio — differently, leading to uncorrelated changes in the measured δ-values, and, ultimately, to a drift in the $\Delta'^{17}O$ values.

Figure 5 shows a 10-hour measurement of a CO_2-in-air mixture using TILDAS made at the University of Göttingen (cf. Fig. 3 in Bajnai et al. (2023)). In this prototype setup, the thermal destabilization led to a 0.04 K variation in the cell temperature (Fig. 5a), closely tracking fluctuations in the laboratory's ambient temperature. Although the optical cell temperature is regulated by a recirculating water chiller, this system cannot fully compensate for rapid or large temperature changes. The 0.04 K temperature variation is broadly reflected in the measured concentrations of the "626", "627", and "628" isotopologues. However, these changes are not identically mirrored across the three isotopologue concentrations (Fig. 5b), leading to uncorrelated variations in the δ-values (Fig. 5c) and resulting in a 1500 ppm drift in the $\Delta'^{17}O$ values (Fig. 5d).

Due to the empirical nature of the line shape fitting, variations in the analytical conditions can introduce instrumental drift. Instrumental drift is mitigated by bracketing each sample analysis with measurements of a working standard (McKinney et al., 1950). This approach relies on the assumption that changes in analytical conditions affect both the sample and the standard equally. It also assumes that the changeover between cycles is fast enough for variations in analytical parameters to be approximated by a linear trend between two standard cycles. The internal error of a single replicate analysis, i.e., the repeatability of approximately 10 sample cycles within a bracketing measurement, primarily depends on how constant the measurement conditions, e.g., cell temperature, remain between cycles.

We assess the variability and stability of key analytical parameters — cell temperature, cell pressure, and the mixing ratio of the most abundant CO_2 isotopologue (χ'_{626}) — using four indicators. First, we determined the mean value of each parameter separately for sample and reference cycles within each replicate. Second, we used the range of these parameter means across replicates as a measure of long-term drift in analytical conditions. Third, to quantify systematic deviations between sample and reference measurements, we calculated, for each sample cycle, the difference between its mean value and the mean of the reference cycles immediately before and after. The average of these differences (sample minus reference) is referred to as the mismatch parameter. A mismatch may not decrease the repeatability if, for example it is constant over the cycles of a replicate analyses. However, variations in mismatch values, both within a single replicate and across replicates, affects measurement repeatability. Thus, finally, to assess the short-term stability in the analytical conditions, we calculated the standard deviation of the mismatch values within a replicate.

Figure 6 shows the relationship between the stability of the mismatch in cell temperature, cell pressure, and the mixing ratio of the most abundant CO_2 isotopologue, and the internal repeatability (68% confidence interval) of individual replicate

https://doi.org/10.5194/egusphere-2025-3040
Preprint. Discussion started: 14 August 2025

measurements, each consisting of approximately 10 sample cycles bracketed by working standard analyses. At the University of Göttingen, the temperature mismatch across the cycles of a single replicate remains stable within ±1 mK (Fig. 6a). The cell pressure mismatch stays stable within ±0.8 Pa (approximately ±6 mTorr; Fig. 6c), and the χ'_{626} mismatch within ±1 µmol mol^{-1} (Fig. 6e). None of these parameters show a statistically significant correlation with the observed internal repeatability, suggesting that these variables are kept stable enough during a replicate measurement to avoid influencing the results.

At the University of Cape Town, the across the cycles of a single replicate the mismatch in cell temperature, cell pressure, and χ'_{626} remain stable better than ±3 mK (Fig. 6b), 34.7 Pa (approximately ±260 mTorr; Fig. 6d) ±11.8 µmol mol^{-1} (Fig. 6f), respectively. Weak correlations (up to $R^2 = 0.2$) between the mismatch stabilities and the internal repeatability appear to be driven by outlier points. When considering only the 90% of data with the lowest mismatch stability values, these correlations become statistically insignificant. This suggests that a temperature stability of ±1 mK, a pressure stability of ±10 Pa, and a χ'_{626} stability of ±1 µmol mol^{-1} are sufficient during a replicate measurements to prevent any systematic impact on internal repeatability.

3.4 Long-term variations in the analytical parameters

The external reproducibility of a sample — i.e. the consistency of results across multiple independent replicate analyses — primarily depends on the stability of measurement conditions. Rather than focusing on the drift of individual reference materials, we examine the difference in measured $\Delta'^{17}O$ values between two reference materials. We refer to this difference as compression, adopting terminology similar to that used in mass spectrometry. This approach offers two key advantages: it simplifies the identification of trends in the data and, more importantly, directly relates to the most common isotope standardization strategy, which relies on two-point calibration using reference materials measured within a defined period. In this context, drift in compression directly affects the accuracy of the final $\Delta'^{17}O$ values.

Figure 7 shows the drift over time in the measured $\Delta'^{17}O$ values of two internal standards, χ'_{626}, cell pressure, cell temperature, and the resulting compression in the University of Göttingen dataset. A LOESS fit is used to approximate temporal trends in each variable. To assess which variables most strongly influence compression drift, we performed a multiple linear regression analysis. The resulting R^2 values (Fig. 8a) indicate that cell temperature and pressure are the primary drivers of compression. Including χ'_{626} in the regression model does not significantly improve the model fit. This result is consistent with expectations: given the χ'_{626} sensitivity of $\Delta'^{17}O$ of 6 ppm per µmol mol^{-1}, the observed ca. 2.5 µmol mol^{-1} variation in χ'_{626} would lead to a maximum drift of about 15 ppm, that is comparable to the 1σ repeatability of measurements under ideal conditions. By contrast, the observed ~60 Pa variation in cell pressure and ~0.1 K variation in cell temperature produce more substantial effects on compression.

https://doi.org/10.5194/egusphere-2025-3040
Preprint. Discussion started: 14 August 2025

Figure 9 presents the corresponding data from the University of Cape Town. In this case, χ'_{626} is not considered, as $\Delta'^{17}O$ values have already been corrected to a constant χ'_{626} value of 421 µmol mol^{-1}. Similar to the Göttingen results, multiple linear regression indicates that variations in cell temperature and pressure are the dominant contributors to compression drift (Fig 8b).

3.5 Gas purity

A major advantage of optical isotope ratio measurement techniques over mass spectrometry is that they are inherently free from isobaric interferences. However, optical measurements can still be affected by contaminants, particularly gases that exhibit overlapping absorption features or contribute to peak broadening.

In the spectral window used for triple oxygen isotope analyses of CO_2, the three relevant CO_2 isotopologues produce distinct absorption peaks (Fig. 1), with no overlapping signals from water or other common contaminant gases such as N_2O, NO_2, CO, or SO_2 (c.f., Gordon et al., 2022). For completeness, we note that this advantage does not extend to Δ_{47} clumped isotope analyses, where N_2O exhibit peaks within the relevant spectral window (Yanay et al., 2025). In such cases, a robust sample purification is required to remove interfering species.

The absence of direct spectral overlap does not imply that analyte purity is irrelevant. Variations in the gas composition — particularly the presence of water vapor — can lead to peak broadening effects, as well as isotopic exchange between CO_2 and water. Corresponding changes in the measured molar concentrations, in turn, contribute to variability in isotope ratios across replicate analyses. This effect has been well documented in atmospheric CO_2 monitoring studies (e.g., Paul et al., 2020; Tuzson et al., 2008), and may also be relevant for analyses of CO_2 produced by the acid digestion of carbonates. Although the water content of the released CO_2 analyte is typically low, it is not negligible and may vary depending on acid temperature and density (c.f. Wacker et al., 2013).

An additional source of gas-purity-related error arises when the gas matrices of the sample and reference differ. For example, the spectroscopic fitting parameters used by the Aerodyne Research Inc. TDLWintel software are based on HITRAN data, which assume peak broadening due to collisions in a CO_2-free air matrix. If the actual matrix deviates substantially from this assumption, spectral fits may degrade. This was demonstrated by Bajnai et al. (2023), who observed fitting issues when using Argon as a bathing gas without adjusting the fit parameters. Such matrix effects can also influence the scaling factors a and b in Eqs. (6–9), potentially introducing additional variability into isotope ratio measurements. These discrepancies may become a significant source of uncertainty in air monitoring studies, particularly when the reference gas matrix differs from that of the sample analyte (e.g., CO_2-in-N_2 vs. CO_2-in-air), since the resulting scale offsets can differ and be difficult to correct.

4 Summary and recommendations

Variations in analytical conditions — such as cell temperature, pressure, and the pCO_2 of the analytes — can influence the measured $\Delta'^{17}O$ values. For instance, the sensitivity of $\Delta'^{17}O$ to changes in analyte pCO_2 is approximately ±6 ppm per

https://doi.org/10.5194/egusphere-2025-3040
Preprint. Discussion started: 14 August 2025

µmol mol^{-1}, depending on the instrumentation. This source of bias is particularly relevant for atmospheric monitoring studies, as atmospheric CO_2 concentrations can fluctuate by more than 100 µmol mol^{-1} over the course of a day, potentially causing a drift of over 600 ppm in the measured $\Delta'^{17}O$ values.

In addition to pCO_2, instability in cell temperature and pressure can compromise measurement repeatability. Data from the University of Göttingen and the University of Cape Town show that maintaining cell temperature and pressure stability within ±1 mK and ±10 Pa, respectively, across the cycles of a replicate measurement is sufficient to avoid any resolvable impact on the internal repeatability. To minimize the influence of ambient temperature fluctuations, TILDAS systems are typically placed in thermally insulated enclosures or operated in climate-controlled laboratories.

Long-term drifts in analytical conditions — such as a gradual temperature change of 0.5 K over the course of a year — can compromise the long-term repeatability of measurements. If left unrecognized, these drifts may be misinterpreted as genuine seasonal variations in $\Delta'^{17}O$ data. Continuous monitoring and reporting of the analytical conditions are therefore essential to ensure data integrity over extended timescales.

Finally, we demonstrated that changes in analytical conditions can impact the instrument's scaling, that is, the measured $\Delta'^{17}O$ difference between two standards. To ensure accurate data correction, standards must be measured under identical conditions of temperature and pressure as the samples they are used to correct.

5 Code and data availability

All data and codes used in this manuscript are deposited at GitHub (https://github.com/davidbajnai/TILDAS_drift) and Zenodo (https://doi.org/10.5281/zenodo.15742110) (Bajnai and Hare, 2025). The supplementary files include Table S1 (long-term replicate-level measurement data from the University of Göttingen), Table S2 (long-term replicate-level measurement data from the University of Cape Town), Table S3 (concentration experiments from the University of Cape Town), and Table S4 (concentration experiments from the University of Göttingen).

6 Author contribution

David Bajnai: Conceptualization, Formal analyses, Investigation Methodology, Writing – original draft, Visualization

Vincent J. Hare: Conceptualization, Formal analyses, Investigation Methodology, Writing – original draft

7 Competing interests

The authors declare that they have no conflict of interest.

https://doi.org/10.5194/egusphere-2025-3040
Preprint. Discussion started: 14 August 2025

8 Acknowledgements

David Bajnai gratefully acknowledges Prof. Andreas Pack, head of the stable isotope laboratory at the University of Göttingen, for his generous support and for providing the infrastructure that made this research possible. He also thanks Dennis Kohl and Tommaso Di Rocco for their technical assistance. Vincent Hare gratefully acknowledges the laboratory assistance of Drake Yarian, and Anna Kudriavtseva at the University of Cape Town.

9 Financial support

This work was supported by the Department of Science and Innovation (Republic of South Africa), through funding from the Biogeochemistry Research Infrastructure Platform (BIOGRIP).

10 References

Adnew, G. A., Hofmann, M. E. G., Paul, D., Laskar, A., Surma, J., Albrecht, N., Pack, A., Schwieters, J., Koren, G., Peters, W., and Röckmann, T.: Determination of the triple oxygen and carbon isotopic composition of CO_2 from atomic ion fragments formed in the ion source of the 253 Ultra high-resolution isotope ratio mass spectrometer, Rapid Commun. Mass Spectrom., 33, 1363–1380, https://doi.org/10.1002/rcm.8478, 2019.

Affek, H. P., Vieten, R., Barkan, E., Levi, Y., Ayalon, A., Bar-Matthews, M., Fishman, E., and Assor, A.: $^{17}O_{excess}$ in speleothem carbonates in Soreq Cave as an archive for hydro-climatic conditions, Earth Planet. Sci. Lett., 621, 118366, https://doi.org/10.1016/j.epsl.2023.118366, 2023.

Arduin-Rode, F., Sosa, G., van den Kerkhof, A., Krüger, Y., Bajnai, D., Pack, A., Di Rocco, T., Oyhantçabal, P., Wemmer, K., Herwartz, D., Klipsch, S., Wiegand, B., Siegesmund, S., and Hueck, M.: World-class amethyst-agate geodes from Los Catalanes, Uruguay: Genetic implications from fluid inclusions and stable isotopes, Miner. Deposita, https://doi.org/10.1007/s00126-024-01310-2, 2024.

Bajnai, D. and Hare, V. J.: Supplementary material for: Sensitivity of tunable infrared laser spectroscopic measurements of $\Delta'^{17}O$ in CO_2 to analytical conditions [data set], https://doi.org/10.5281/zenodo.11277153, 2025.

Bajnai, D., Pack, A., Arduin Rode, F., Seefeld, M., Surma, J., and Di Rocco, T.: A dual inlet system for laser spectroscopy of triple oxygen isotopes in carbonate-derived and air CO_2, Geochem. Geophys. Geosyst., 24, e2023GC010976, https://doi.org/10.1029/2023GC010976, 2023.

Bajnai, D., Klipsch, S., Davies, A. J., Raddatz, J., Gischler, E., Rüggeberg, A., Pack, A., and Herwartz, D.: Correcting for vital effects in coral carbonate using triple oxygen isotopes, Geochem. Persp. Let., 31, 38–43, https://doi.org/10.7185/geochemlet.2430, 2024.

Barkan, E. and Luz, B.: High-precision measurements of $^{17}O/^{16}O$ and $^{18}O/^{16}O$ ratios in CO_2, Rapid Commun. Mass Spectrom., 26, 2733–2738, https://doi.org/10.1002/rcm.6400, 2012.

https://doi.org/10.5194/egusphere-2025-3040
Preprint. Discussion started: 14 August 2025

Brand, W. A., Assonov, S. S., and Coplen, T. B.: Correction for the ^{17}O interference in $\delta(^{13}C)$ measurements when analyzing CO_2 with stable isotope mass spectrometry (IUPAC Technical Report), Pure Appl. Chem., 82, 1719–1733, https://doi.org/10.1351/pac-rep-09-01-05, 2010.

Brenninkmeijer, C. A. M. and Röckmann, T.: A rapid method for the preparation of O_2 from CO_2 for mass spectrometric measurement of $^{17}O/^{16}O$ ratios, Rapid Commun. Mass Spectrom., 12, 479–483, https://doi.org/10.1002/(SICI)1097-0231(19980430)12:8<479::AID-RCM184>3.0.CO;2-R, 1998.

Chaillot, J., Kassi, S., Clauzel, T., Pesnin, M., Casado, M., Landais, A., and Daëron, M.: Linking the oxygen-17 compositions of water and carbonate reference materials using infrared absorption spectroscopy of carbon dioxide, Chem. Geol., 673, 122450, https://doi.org/10.1016/j.chemgeo.2024.122450, 2025.

Craig, H.: Isotopic standards for carbon and oxygen and correction factors for mass-spectrometric analysis of carbon dioxide, Geochim. Cosmochim. Acta, 12, 133–149, https://doi.org/10.1016/0016-7037(57)90024-8, 1957.

De Biévre, P., Gallet, M., Holden, N. E., and Barnes, I. L.: Isotopic abundances and atomic weights of the elements, J. Phys. Chem. Ref. Data, 13, 809–891, https://doi.org/10.1063/1.555720, 1984.

Gordon, I. E., Rothman, L. S., Hargreaves, R. J., Hashemi, R., Karlovets, E. V., Skinner, F. M., Conway, E. K., Hill, C., Kochanov, R. V., Tan, Y., Wcisło, P., Finenko, A. A., Nelson, K., Bernath, P. F., Birk, M., Boudon, V., Campargue, A., Chance, K. V., Coustenis, A., Drouin, B. J., Flaud, J. –M., Gamache, R. R., Hodges, J. T., Jacquemart, D., Mlawer, E. J., Nikitin, A. V., Perevalov, V. I., Rotger, M., Tennyson, J., Toon, G. C., Tran, H., Tyuterev, V. G., Adkins, E. M., Baker, A., Barbe, A., Canè, E., Császár, A. G., Dudaryonok, A., Egorov, O., Fleisher, A. J., Fleurbaey, H., Foltynowicz, A., Furtenbacher, T., Harrison, J. J., Hartmann, J. –M., Horneman, V. –M., Huang, X., Karman, T., Karns, J., Kassi, S., Kleiner, I., Kofman, V., Kwabia–Tchana, F., Lavrentieva, N. N., Lee, T. J., Long, D. A., Lukashevskaya, A. A., Lyulin, O. M., Makhnev, V. Yu., Matt, W., Massie, S. T., Melosso, M., Mikhailenko, S. N., Mondelain, D., Müller, H. S. P., Naumenko, O. V., Perrin, A., Polyansky, O. L., Raddaoui, E., Raston, P. L., Reed, Z. D., Rey, M., Richard, C., Tóbiás, R., Sadiek, I., Schwenke, D. W., Starikova, E., Sung, K., Tamassia, F., Tashkun, S. A., Vander Auwera, J., Vasilenko, I. A., Vigasin, A. A., Villanueva, G. L., Vispoel, B., Wagner, G., Yachmenev, A., and Yurchenko, S. N.: The HITRAN2020 molecular spectroscopic database, Journal of Quantitative Spectroscopy and Radiative Transfer, 277, 107949, https://doi.org/10.1016/j.jqsrt.2021.107949, 2022.

Griffith, D. W. T., Deutscher, N. M., Caldow, C., Kettlewell, G., Riggenbach, M., and Hammer, S.: A Fourier transform infrared trace gas and isotope analyser for atmospheric applications, Atmos. Meas. Tech., 5, 2481–2498, https://doi.org/10.5194/amt-5-2481-2012, 2012.

Hare, V. J., Dyroff, C., Nelson, D. D., and Yarian, D. A.: High-precision triple oxygen isotope analysis of carbon dioxide by tunable infrared laser absorption spectroscopy, Anal. Chem., 94, 16023–16032, https://doi.org/10.1021/acs.analchem.2c03005, 2022.

Hare, V. J., Yarian, D. A., Faith, J. T., Harris, C., Lee-Thorp, J. A., Passey, B. H., Sokolowski, K. G., and Ségalen, L.: Triple oxygen isotopes in eggshell carbonate as a proxy of late Cenozoic CO_2 and primary productivity, Geochim. Cosmochim. Acta, S0016703725001826, https://doi.org/10.1016/j.gca.2025.04.002, 2025.

Hoag, K. J., Still, C. J., Fung, I. Y., and Boering, K. A.: Triple oxygen isotope composition of tropospheric carbon dioxide as a tracer of terrestrial gross carbon fluxes, Geophys. Res. Lett., 32, L02802, https://doi.org/10.1029/2004GL021011, 2005.

Hofmann, M. E. and Pack, A.: Technique for high-precision analysis of triple oxygen isotope ratios in carbon dioxide, Anal. Chem., 82, 4357–61, https://doi.org/10.1021/ac902731m, 2010.

https://doi.org/10.5194/egusphere-2025-3040
Preprint. Discussion started: 14 August 2025

Horváth, B., Hofmann, M. E. G., and Pack, A.: On the triple oxygen isotope composition of carbon dioxide from some combustion processes, Geochim. Cosmochim. Acta, 95, 160–168, https://doi.org/10.1016/j.gca.2012.07.021, 2012.

Kelson, J. R., Petersen, S. V., Niemi, N. A., Passey, B. H., and Curley, A. N.: Looking upstream with clumped and triple oxygen isotopes of estuarine oyster shells in the early Eocene of California, USA, Geology, 50, 755–759, https://doi.org/10.1130/G49634.1, 2022.

Koren, G., Schneider, L., Velde, I. R., Schaik, E., Gromov, S. S., Adnew, G. A., Mrozek Martino, D. J., Hofmann, M. E. G., Liang, M., Mahata, S., Bergamaschi, P., Laan-Luijkx, I. T., Krol, M. C., Röckmann, T., and Peters, W.: Global 3-D simulations of the triple oxygen isotope signature $\Delta^{17}O$ in atmospheric CO_2, J. Geophys. Res. Atmos., 124, 8808–8836, https://doi.org/10.1029/2019JD030387, 2019.

Liang, M.-C., Laskar, A. H., Barkan, E., Newman, S., Thiemens, M. H., and Rangarajan, R.: New constraints of terrestrial and oceanic global gross primary productions from the triple oxygen isotopic composition of atmospheric CO_2 and O_2, Sci Rep, 13, 2162, https://doi.org/10.1038/s41598-023-29389-z, 2023.

Luz, B. and Barkan, E.: Variations of $^{17}O/^{16}O$ and $^{18}O/^{16}O$ in meteoric waters, Geochim. Cosmochim. Acta, 74, 6276–6286, https://doi.org/10.1016/j.gca.2010.08.016, 2010.

Mahata, S., Bhattacharya, S. K., Wang, C.-H., and Liang, M.-C.: An improved CeO_2 method for high-precision measurements of $^{17}O/^{16}O$ ratios for atmospheric carbon dioxide: High-precision triple-isotope measurements of CO_2, Rapid Commun. Mass Spectrom., 26, 1909–1922, https://doi.org/10.1002/rcm.6296, 2012.

Mahata, S., Bhattacharya, S. K., Wang, C. H., and Liang, M. C.: Oxygen isotope exchange between O_2 and CO_2 over hot platinum: An innovative technique for measuring $\Delta^{17}O$ in CO_2, Anal. Chem., 85, 6894–6901, https://doi.org/10.1021/ac4011777, 2013.

Matsuhisa, Y., Goldsmith, J. R., and Clayton, R. N.: Mechanisms of hydrothermal crystallization of quartz at 250°C and 15 kbar, Geochim. Cosmochim. Acta, 42, 173–182, https://doi.org/10.1016/0016-7037(78)90130-8, 1978.

McCrea, J. M.: On the Isotopic Chemistry of Carbonates and a Paleotemperature Scale, J. Chem. Phys., 18, 849–857, https://doi.org/10.1063/1.1747785, 1950.

McKinney, C. R., McCrea, J. M., Epstein, S., Allen, H. A., and Urey, H. C.: Improvements in mass spectrometers for the measurement of small differences in isotope abundance ratios, Rev. Sci. Instrum., 21, 724–730, https://doi.org/10.1063/1.1745698, 1950.

McManus, J. B., Nelson, D. D., Shorter, J. H., Jimenez, R., Herndon, S., Saleska, S., and Zahniser, M.: A high precision pulsed quantum cascade laser spectrometer for measurements of stable isotopes of carbon dioxide, J. Mod. Opt., 52, 2309–2321, https://doi.org/10.1080/09500340500303710, 2006.

McManus, J. B., Zahniser, M. S., Nelson, D. D., Shorter, J. H., Herndon, S. C., Jervis, D., Agnese, M., McGovern, R., Yacovitch, T. I., and Roscioli, J. R.: Recent progress in laser-based trace gas instruments: performance and noise analysis, Appl. Phys. B, 119, 203–218, https://doi.org/10.1007/s00340-015-6033-0, 2015.

Miller, M. F., Pack, A., Bindeman, I. N., and Greenwood, R. C.: Standardizing the reporting of $\Delta'^{17}O$ data from high precision oxygen triple-isotope ratio measurements of silicate rocks and minerals, Chem. Geol., 532, 119332, https://doi.org/10.1016/j.chemgeo.2019.119332, 2020.

https://doi.org/10.5194/egusphere-2025-3040
Preprint. Discussion started: 14 August 2025

Mohn, J., Wolf, B., Toyoda, S., Lin, C.-T., Liang, M.-C., Brüggemann, N., Wissel, H., Steiker, A. E., Dyckmans, J., Szwec, L., Ostrom, N. E., Casciotti, K. L., Forbes, M., Giesemann, A., Well, R., Doucett, R. R., Yarnes, C. T., Ridley, A. R., Kaiser, J., and Yoshida, N.: Interlaboratory assessment of nitrous oxide isotopomer analysis by isotope ratio mass spectrometry and laser spectroscopy: current status and perspectives: Interlaboratory assessment of nitrous oxide isotopomer analysis, Rapid Commun. Mass Spectrom., 28, 1995–2007, https://doi.org/10.1002/rcm.6982, 2014.

Nataraj, A., Gianella, M., Prokhorov, I., Tuzson, B., Bertrand, M., Mohn, J., Faist, J., and Emmenegger, L.: Quantum cascade laser absorption spectrometer with a low temperature multipass cell for precision clumped CO_2 measurement, Opt. Express, 30, 4631, https://doi.org/10.1364/OE.447172, 2022.

Nelson, D. D., McManus, J. B., Herndon, S. C., Zahniser, M. S., Tuzson, B., and Emmenegger, L.: New method for isotopic ratio measurements of atmospheric carbon dioxide using a 4.3 μm pulsed quantum cascade laser, Appl. Phys. B, 90, 301–309, https://doi.org/10.1007/s00340-007-2894-1, 2008.

Passey, B. H., Hu, H., Ji, H., Montanari, S., Li, S., Henkes, G. A., and Levin, N. E.: Triple oxygen isotopes in biogenic and sedimentary carbonates, Geochim. Cosmochim. Acta, 141, 1–25, https://doi.org/10.1016/j.gca.2014.06.006, 2014.

Paul, D., Scheeren, H. A., Jansen, H. G., Kers, B. A. M., Miller, J. B., Crotwell, A. M., Michel, S. E., Gatti, L. V., Domingues, L. G., Correia, C. S. C., Neves, R. A. L., Meijer, H. A. J., and Peters, W.: Evaluation of a field-deployable Nafion™-based air-drying system for collecting whole air samples and its application to stable isotope measurements of CO_2, Atmos. Meas. Tech., 13, 4051–4064, https://doi.org/10.5194/amt-13-4051-2020, 2020.

Perdue, N., Sharp, Z., Nelson, D., Wehr, R., and Dyroff, C.: A rapid high-precision analytical method for triple oxygen isotope analysis of CO_2 gas using tunable infrared laser direct absorption spectroscopy, Rapid Commun. Mass Spectrom., 36, e9391, https://doi.org/10.1002/rcm.9391, 2022.

Petersen, S. V., Defliese, W. F., Saenger, C., Daëron, M., Huntington, K. W., John, C. M., Kelson, J. R., Coleman, A. S., Kluge, T., Olack, G. A., Schauer, A. J., Bajnai, D., Bonifacie, M., Breitenbach, S. F., Fiebig, J., Fernandez, A. B., Henkes, G. A., Hodell, D., Katz, A., Kele, S., Lohmann, K. C., Passey, B. H., Peral, M. Y., Petrizzo, D. A., Rosenheim, B. E., Tripati, A., Venturelli, R., Young, E. D., and Winkelstern, I. Z.: Effects of improved ^{17}O correction on interlaboratory agreement in clumped isotope calibrations, estimates of mineral-specific offsets, and temperature dependence of acid digestion fractionation, Geochem. Geophys. Geosyst., 20, 3495–3519, https://doi.org/10.1029/2018gc008127, 2019.

Prokhorov, I., Kluge, T., and Janssen, C.: Laser absorption spectroscopy of rare and doubly substituted carbon dioxide isotopologues, Anal. Chem., 91, 15491–15499, https://doi.org/10.1021/acs.analchem.9b03316, 2019.

Sakai, S., Matsuda, S., Hikida, T., Shimono, A., McManus, J. B., Zahniser, M., Nelson, D., Dettman, D. L., Yang, D., and Ohkouchi, N.: High-precision simultaneous $^{18}O/^{16}$ O, $^{13}C/^{12}$ C, and $^{17}O/^{16}O$ analyses for microgram quantities of $CaCO_3$ by tunable infrared laser absorption spectroscopy, Anal. Chem., 89, 11846–11852, https://doi.org/10.1021/acs.analchem.7b03582, 2017.

Sha, L., Dang, H., Wang, Y., Wassenburg, J. A., Baker, J. L., Li, H., Sinha, A., Brahim, Y. A., Wu, N., Lu, Z., Yang, C., Dong, X., Lu, J., Zhang, H., Mahata, S., Cai, Y., Jian, Z., and Cheng, H.: Triple oxygen isotope reveals insolation-forced tropical moisture cycles, Science Advances, 10, eadp7855, https://doi.org/10.1126/sciadv.adp7855, 2024.

Steur, P. M., Scheeren, H. A., Nelson, D. D., McManus, J. B., and Meijer, H. A. J.: Simultaneous measurement of $\delta^{13}C$, $\delta^{18}O$ and $\delta^{17}O$ of atmospheric CO_2 – performance assessment of a dual-laser absorption spectrometer, Atmos. Meas. Tech., 14, 4279–4304, https://doi.org/10.5194/amt-14-4279-2021, 2021.

https://doi.org/10.5194/egusphere-2025-3040
Preprint. Discussion started: 14 August 2025

Steur, P. M., Scheeren, H. A., Koren, G., Adnew, G. A., Peters, W., and Meijer, H. A. J.: Interannual variations in the $\Delta(^{17}O)$ signature of atmospheric CO_2 at two mid-latitude sites suggest a close link to stratosphere-troposphere exchange, Atmos. Chem. Phys., 24, 11005–11027, https://doi.org/10.5194/acp-24-11005-2024, 2024.

Stoltmann, T., Casado, M., Daëron, M., Landais, A., and Kassi, S.: Direct, precise measurements of isotopologue abundance ratios in CO_2 using molecular absorption spectroscopy: Application to $\Delta^{17}O$, Anal. Chem., 89, 10129–10132, https://doi.org/10.1021/acs.analchem.7b02853, 2017.

Thiemens, M. H., Chakraborty, S., and Jackson, T. L.: Decadal $\Delta^{17}O$ record of tropospheric CO_2: Verification of a stratospheric component in the troposphere: 10 yr record of $\Delta^{17}O$ of tropospheric CO_2, J. Geophys. Res. Atmos., 119, 6221–6229, https://doi.org/10.1002/2013JD020317, 2014.

Tuzson, B., Mohn, J., Zeeman, M. J., Werner, R. A., Eugster, W., Zahniser, M. S., Nelson, D. D., McManus, J. B., and Emmenegger, L.: High precision and continuous field measurements of $\delta^{13}C$ and $\delta^{18}O$ in carbon dioxide with a cryogen-free QCLAS, Appl. Phys. B, 92, 451–458, https://doi.org/10.1007/s00340-008-3085-4, 2008.

Wacker, U., Fiebig, J., and Schoene, B. R.: Clumped isotope analysis of carbonates: comparison of two different acid digestion techniques, Rapid Commun. Mass Spectrom., 27, 1631–1642, https://doi.org/10.1002/rcm.6609, 2013.

Wang, Z., Nelson, D. D., Dettman, D. L., McManus, J. B., Quade, J., Huntington, K. W., Schauer, A. J., and Sakai, S.: Rapid and precise analysis of carbon dioxide clumped isotopic composition by tunable infrared laser differential spectroscopy, Anal. Chem., 92, 2034–2042, https://doi.org/10.1021/acs.analchem.9b04466, 2020.

Wostbrock, J. A. G., Cano, E. J., and Sharp, Z. D.: An internally consistent triple oxygen isotope calibration of standards for silicates, carbonates and air relative to VSMOW2 and SLAP2, Chem. Geol., 533, 119432, https://doi.org/10.1016/j.chemgeo.2019.119432, 2020.

Wostbrock, J. A. G., Witts, J. D., Gao, Y., Peshek, C., Myers, C. E., Henkes, G., and Sharp, Z. D.: Reconstructing paleoenvironments of the Late Cretaceous Western Interior Seaway, USA, using paired triple oxygen and carbonate clumped isotope measurements, Geol. Soc. Am. Bull., https://doi.org/10.1130/B37543.1, 2024.

Yanay, N., Wang, Z., Dettman, D. L., Quade, J., Huntington, K. W., Schauer, A. J., Nelson, D. D., McManus, J. B., Thirumalai, K., Sakai, S., Rebaza Morillo, A., and Mallik, A.: Rapid and precise measurement of carbonate clumped isotopes using laser spectroscopy, Sci. Adv., 8, eabq0611, https://doi.org/10.1126/sciadv.abq0611, 2022.

Yanay, N., Quade, J., Wang, Z., Waseem, M. T., and Dettman, D. L.: Alteration of carbonate clumped isotope composition by burial heating in foreland sediments of the Himalaya, Geochim. Cosmochim. Acta, 394, 15–31, https://doi.org/10.1016/j.gca.2025.02.023, 2025.

Young, E. D., Galy, A., and Nagahara, H.: Kinetic and equilibrium mass-dependent isotope fractionation laws in nature and their geochemical and cosmochemical significance, Geochim. Cosmochim. Acta, 66, 1095–1104, https://doi.org/10.1016/s0016-7037(01)00832-8, 2002.

Zhang, N., Prokhorov, I., Kueter, N., Li, G., Tuzson, B., Magyar, P. M., Ebert, V., Sivan, M., Nakagawa, M., Gilbert, A., Ueno, Y., Yoshida, N., Röckmann, T., Bernasconi, S. M., Emmenegger, L., and Mohn, J.: Rapid high-sensitivity analysis of methane clumped isotopes ($\Delta^{13}CH_3D$ and $\Delta^{12}CH_2D_2$) using mid-infrared laser spectroscopy, Anal. Chem., acs.analchem.4c05406, https://doi.org/10.1021/acs.analchem.4c05406, 2025.

https://doi.org/10.5194/egusphere-2025-3040
Preprint. Discussion started: 14 August 2025

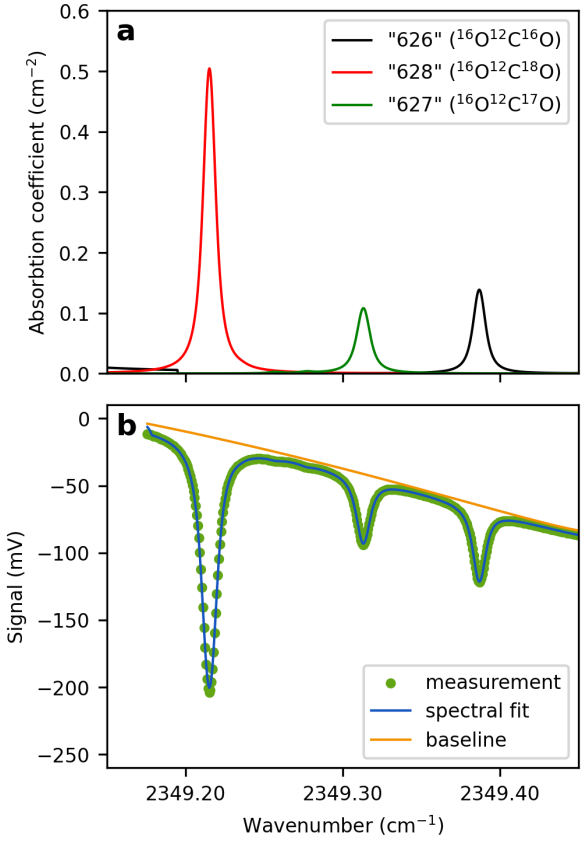

Figure 1. Modeled and measured CO_2 absorption spectra for $\Delta'^{17}O$ analysis

a) Absorption coefficients of the three CO_2 isotopologues used for triple oxygen isotope measurements, retrieved from the HITRAN database. The broadening coefficients reflect the experimental conditions below: $P = 41.335$ Torr, $T = 297.6$ K, and $pCO_2 = 420$ µmol mol^{-1}. b) Measured spectrum of a CO_2-in-air gas mixture obtained using TILDAS. Green dots represent individual data points, each corresponding to an average of 1538 spectra acquired at a rate of one spectrum per second. The TDLWintel software fits the spectrum to the data (blue line), accounting for several parameters, including the analyte's temperature and pressure, as well as spectroscopic information from the HITRAN database. Diluting a pure CO_2 analyte with a collision gas broadens the absorption peaks, allowing each peak to be represented by more data points.

https://doi.org/10.5194/egusphere-2025-3040
Preprint. Discussion started: 14 August 2025

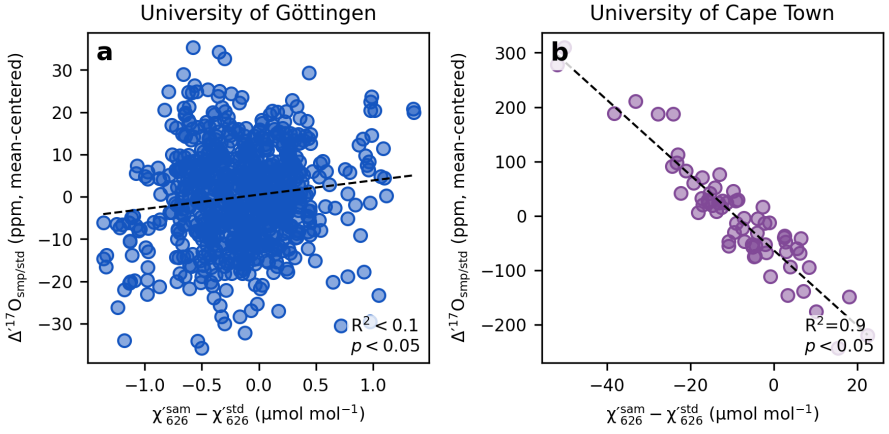

Figure 2. The effect of pCO_2 mismatch between sample and reference on the measured $\Delta'^{17}O$ values.

https://doi.org/10.5194/egusphere-2025-3040
Preprint. Discussion started: 14 August 2025

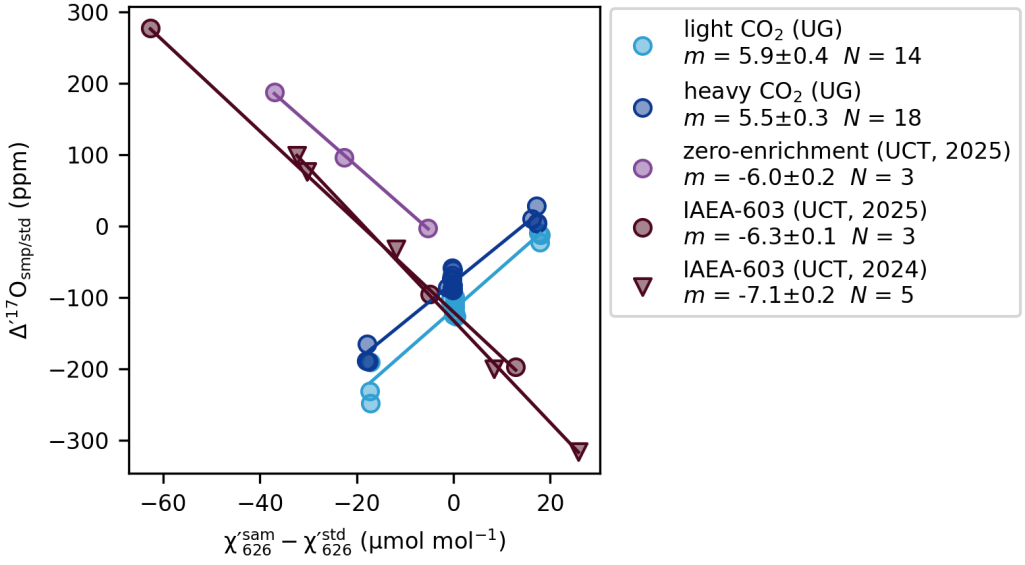

Figure 3. Experiments to determine the concentration dependence of Δ'^{17}O

Mismatches between the measured χ'_{626} mixing ratios of sample and working standards, measured by TILDAS at Cape Town (UCT; purple and brown circles and triangles), and Göttingen (UG; blue circles), are plotted against Δ'^{17}O values. Each data point represents the mean of a dual-inlet bracketing measurement consisting of approximately 10 cycles. IAEA-603 data at UCT were obtained from two separate analytical sessions in 2024 and 2025, which yielded slightly different slopes. Error bars for Δ'^{17}O (68% CI) are smaller than the markers.

https://doi.org/10.5194/egusphere-2025-3040
Preprint. Discussion started: 14 August 2025

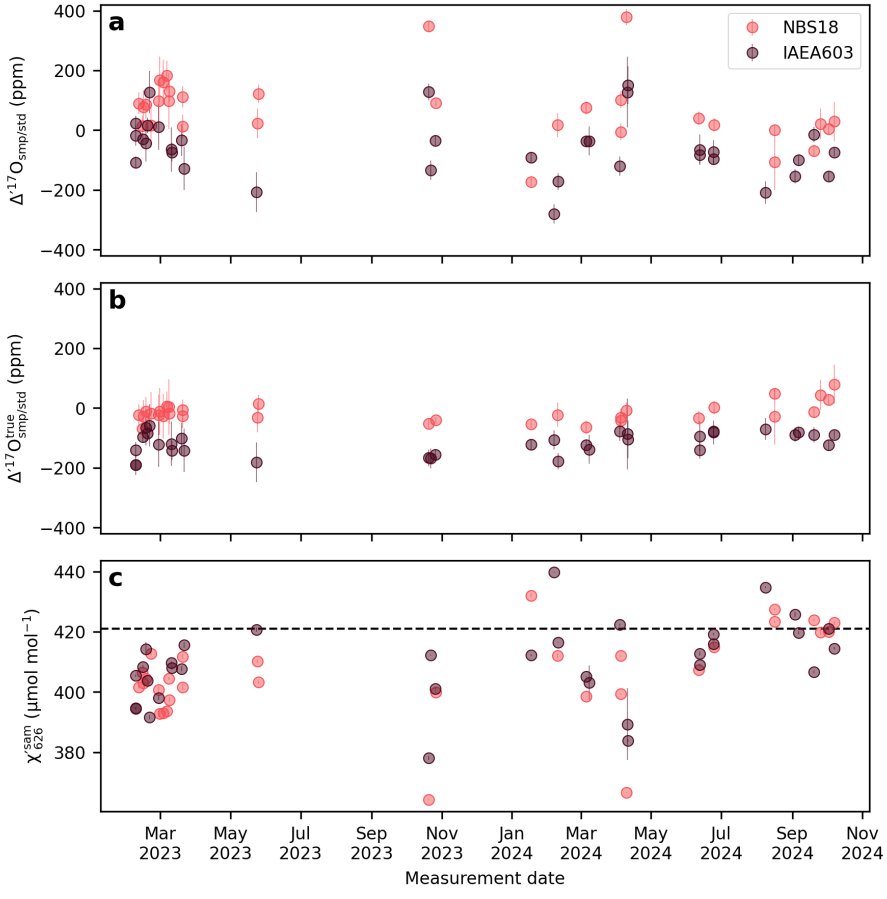

Figure 4. The effect of scale-offset correction of the Cape Town Δ'^{17}O data.

a) Measured Δ'^{17}O values, b) Δ'^{17}O values after scale-offset correction, c) Average χ'_{626} values of the sample gas within a replicate analysis. For the Cape Town setup the χ'_{626} value of the reference gas is constant 421 µmol mol^{-1}, and within a replicate measurement the mismatch between subsequent χ'_{626} values stay within <1 µmol mol^{-1}.

https://doi.org/10.5194/egusphere-2025-3040
Preprint. Discussion started: 14 August 2025

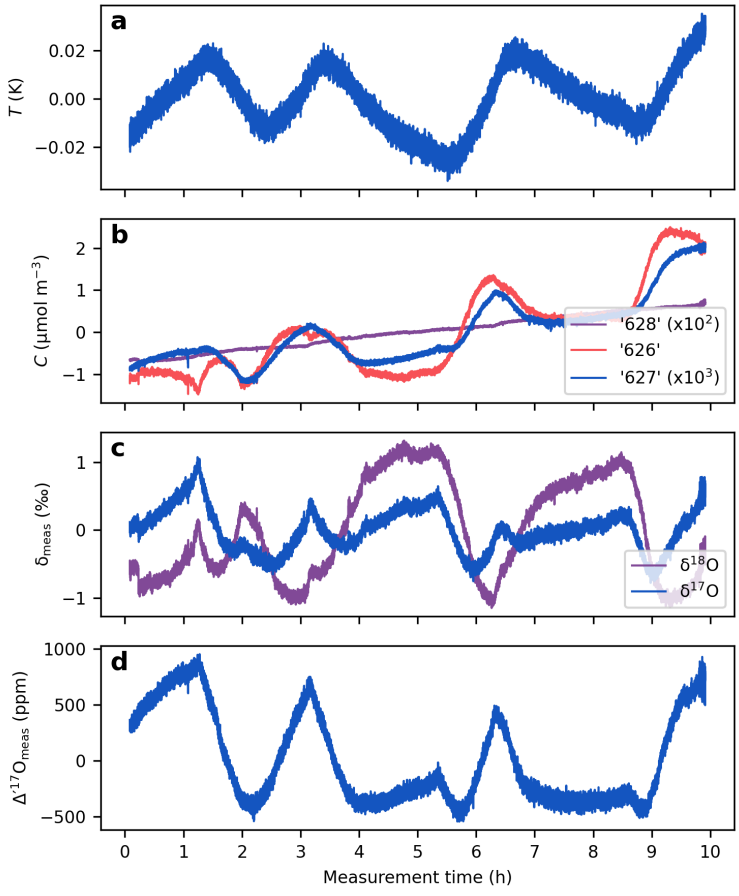

Figure 5. Effect of cell temperature on measured isotope ratios.

The figure shows a continuous measurement of a CO_2-in-air mixture at 420 µmol mol^{-1}. a) Cell temperature; b) Isotopologue concentrations calculated from mixing ratios, cell temperature and cell pressure (Eq. 3); c) δ-values; d) Δ'^{17}O values. All data are mean centered to highlight relative variations.

https://doi.org/10.5194/egusphere-2025-3040
Preprint. Discussion started: 14 August 2025

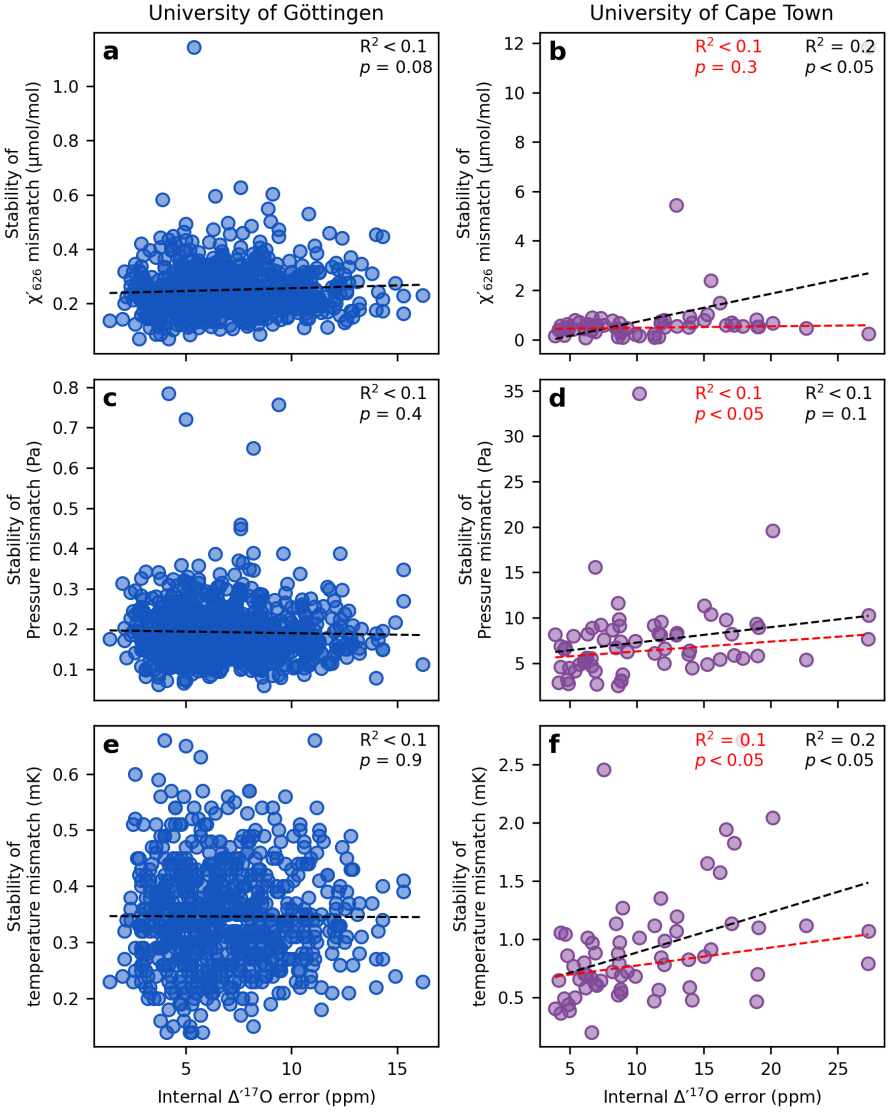

Figure 6. Effect of short-term analytical variability on Δ'^{17}O precision.

The standard deviation of the mismatch parameters serves as a measure of variability in analytical conditions across cycles of individual replicate analyses. The internal repeatability is reported as the 68% confidence interval of the calculated Δ'^{17}O values from approximately 10 sample cycles. The black dashed line and the corresponding correlation coefficients indicate the relationship between parameter stability and internal repeatability. In addition, for the Cape Town data, red dashed lines represent the correlation when only the lowest 90% of the data (based on mismatch variability) is considered. In both laboratory setups, the analytical conditions are generally stable enough that they do not have a detectable effect on the internal reproducibility of the measurements.

https://doi.org/10.5194/egusphere-2025-3040
Preprint. Discussion started: 14 August 2025

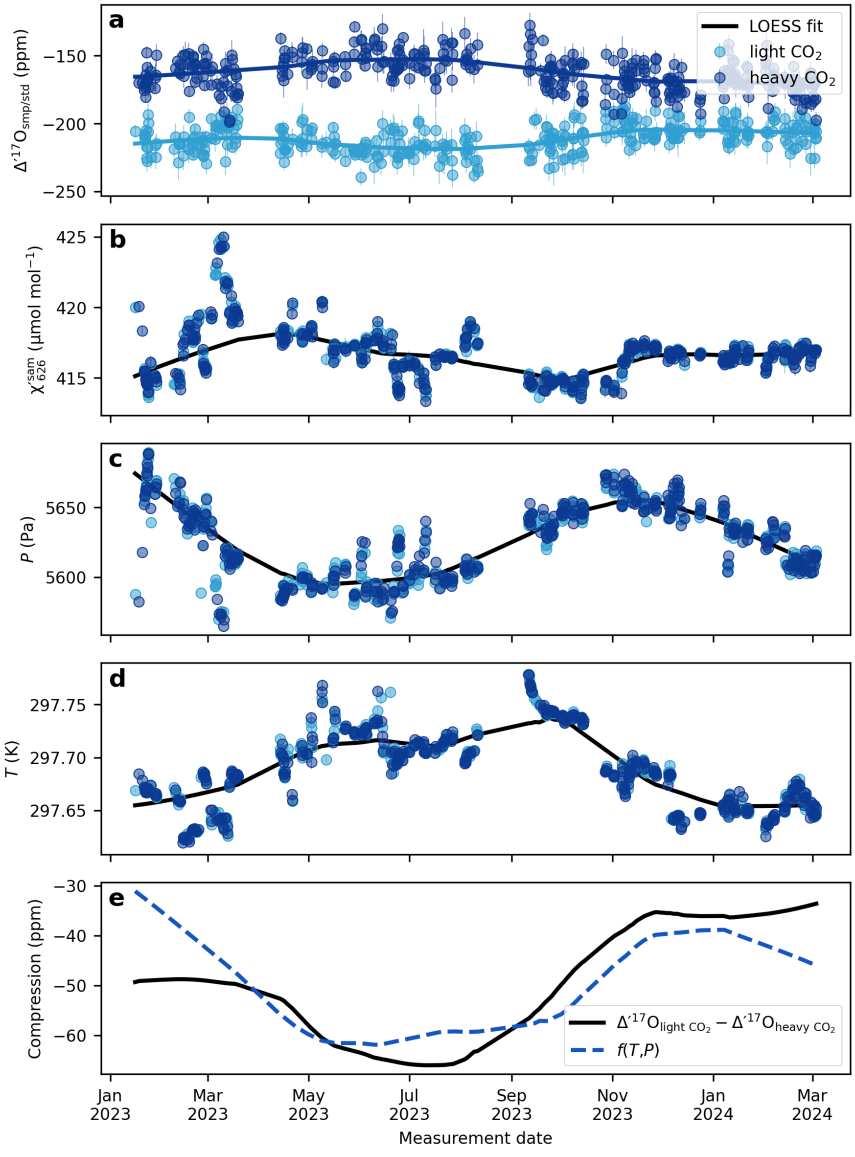

Figure 7. The drift of the compression of the Göttingen setup.

a) $\Delta'^{17}O$ values for the two internal reference gases, light CO_2 and heavy CO_2. b) average χ'_{626} of the sample cycles within a replicate. For the Göttingen setup the χ'_{626} of the reference cycles are within 1 µmol mol^{-1} of the samples. c) cell pressure, d) cell temperature, e) Compression of the system defined as the difference between the $\Delta'^{17}O$ values of the light CO_2 and heavy CO_2. The solid lines depict LOESS fits to the data (smoothing: 0.4). The dashed blue line shows the multivariate linear regression model from the LOESS fits of the cell pressure and the cell temperature.

https://doi.org/10.5194/egusphere-2025-3040
Preprint. Discussion started: 14 August 2025

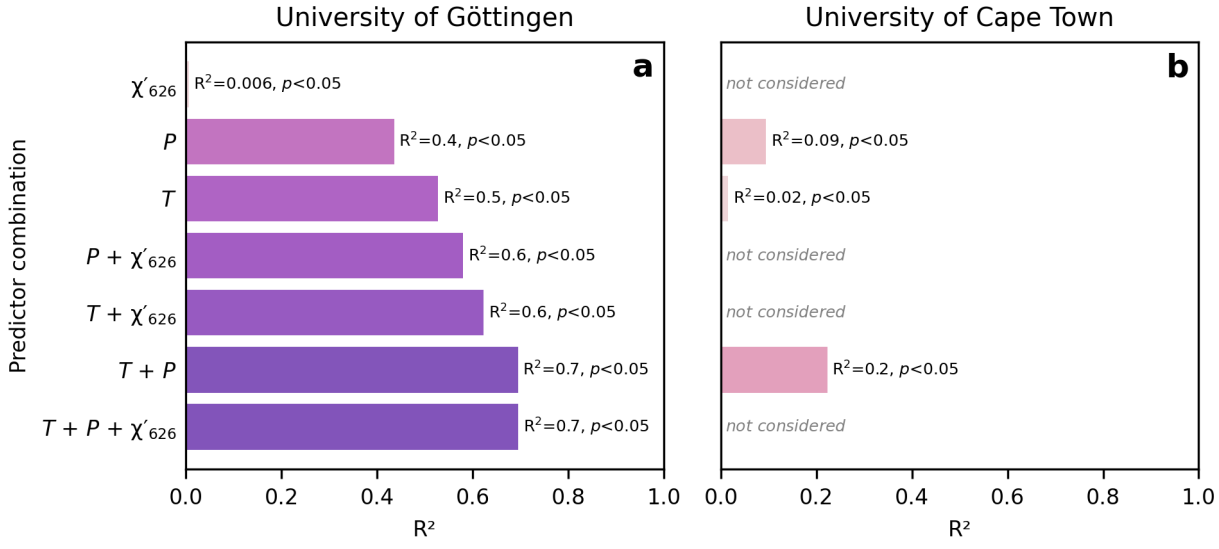

Figure 8. Coefficient of determination (R^2) for multiple linear regression models predicting compression in $\Delta'^{17}O$ from different combinations of cell temperature, cell pressure, and χ'_{626}

a) University of Göttingen, b) University of Cape Town. Here the models use only cell temperature and cell pressure, as the $\Delta'^{17}O$ were already corrected for scale-offset and normalized to a χ'_{626} value of 421 µmol mol^{-1}. The multiple linear regression models using both cell pressure and temperature as predictors are plotted on Figures 7e and 9d. We speculate that the relatively weaker correlation in the UCT dataset is due to the fewer data points used to compute the LOESS fits.

https://doi.org/10.5194/egusphere-2025-3040
Preprint. Discussion started: 14 August 2025

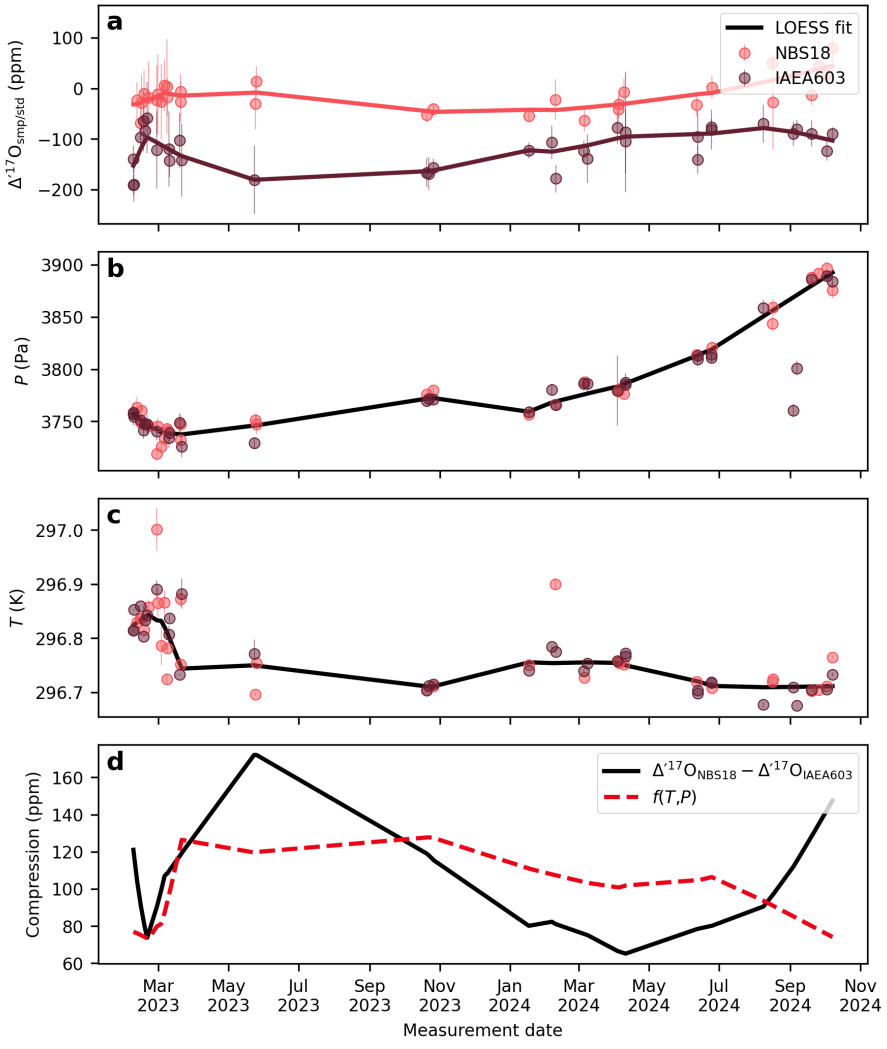

525

Figure 9. The drift of the compression of the Cape Town setup.

a) $\Delta'^{17}O$ values for the two most commonly used reference materials, NBS-18 and IAEA-603 b) cell pressure, c) cell temperature, d) Compression of the system defined as the difference between the $\Delta'^{17}O$ values of NBS-18 and IAEA-603. The dashed red line shows the multivariate linear regression model from the LOESS fits of the cell pressure and the cell
530 temperature.